Convergency of a Leap-Frog Discontinuous Galerkin Method for Solving Time-Domain Maxwell's Equation in Anisotropic Materials

Adérito Araújo, Sílvia Barbeiro , Maryam Khaksar Ghalati

CMUC, Department of Mathematics,
University of Coimbra, Portugal

BIT Circus
Numerical Mathematics and Computational Science
Umeå University, August 26-28, 2015

Outline

- Motivation
  Wave propagation in biological tissue (retina)
- Maxwell's equation in anisotropic material
- Numerical methods
  Stability and convergency of Leap-frog discontinuous Galerkin scheme
- Numerical Results
  Illustrating the high-order convergency

Motivation

Motivation

The motivation of this work has come from the light scattering effects in human retina.

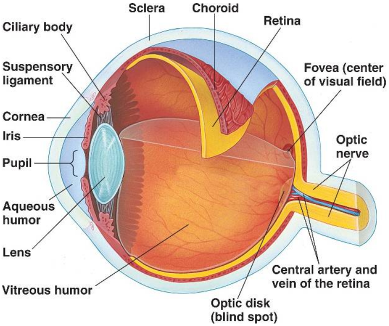

Figure: Human Eye.

Retina

- Thin layer backside of the eye;
  Varies between 0.10 and 0.24 mm along the eye
- Light sensitive part of tissue
- Part of central nervous system;
  Constituted by layers of neurons interconnected through synapses.

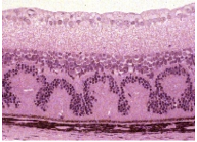

Figure: Histologic image of the retina

Optical Coherence Tomography

- High resolution imaging technique
- Noninvasive
- Analogous to ultrasound imaging, but using light instead of sound
- Based on low coherence interferometry
- Rely on differences in backscattering properties of small volumes within the tissue.
- A useful diagnostic tool in ophtalmologhy

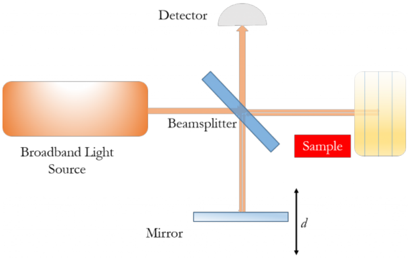

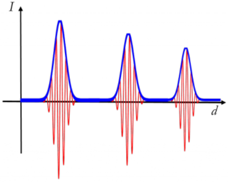

OCT

- A- scan
  When we change the position of the mirror, we get reflections from different depths for the same lateral position.
- B- scan
  If we take multiple A-scans along the same axis, all of them parallel between themselves, we have a bi-dimensional image of retina.

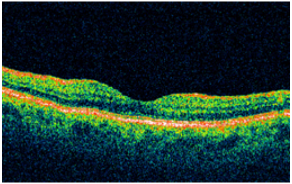

Figure: OCT B- Scan

- OCT has the possibility of evaluating different elements in measuring the retinal nerve fiber layer (RNFL)

Motivation

- Strong correlation between RNFL thinning and a reduction in tissue birefringence
- Waveguides with induced anisotropy may worth to be modeled as they could play a role in biological waveguides

In order to model in detail the behavior of the electromagnetic wave as it travels through the retina we arrive at solving the Maxwell's equations in anisotropic medium. [1]

[1] A. Araújo, S. Barbeiro, L. Pinto, F. Caramelo, A. L. Correia, M. Morgado, P. Serranho, A. S. C. Silva and R. Bernardes, "Maxwell's equations to model electromagnetic wave's propagation through eye's structures", Proceedings of CMMSE 2013, vol. 1, Ian Hamilton and Jesús Vigo-Aguiar Eds., pp. 121-129, 2013.

Maxwell's Equations in Anisotropic Materials

- 2D Maxwell's equations in transverse electric (TE) mode:

$$
\begin{aligned}
\epsilon \frac{\partial E}{\partial t} &= \nabla \times H, \\
\mu \frac{\partial H}{\partial t} &= -\text{curl } E, \qquad \text{in } \Omega \times (0, T].
\end{aligned}
$$

- $E = (E_x, E_y)$
- $H = (H_z)$
- Ω is a two-dimensional domain.
- μ: Isotropic permeability;
- Anisotropic permittivity tensor

$$
\epsilon = \begin{pmatrix} \epsilon_{xx} & \epsilon_{xy} \\ \epsilon_{yx} & \epsilon_{yy} \end{pmatrix}
$$

Boundary condition

- Perfect electric conductor boundary condition (PEC)

$$n \times E = 0, \qquad \text{on } \partial\Omega,$$

- Perfect magnetic conductor boundary condition (PMC)

$$n \times H = 0, \qquad \text{on } \partial\Omega,$$

- Silver-Müller absorbing boundary condition

$$n \times E = c\mu n \times (H_z \times n), \qquad \text{on } \partial\Omega,$$

where we assume the medium is isotropic near the absorbing boundary , i.e.,

$$\epsilon = \begin{pmatrix} \varepsilon & 0 \\ 0 & \varepsilon \end{pmatrix}$$

and the local light speed c is given by $\varepsilon\mu c^2 = 1$.

Numerical Method

- Space discretization:
  Nodal Discontinuous Galerkin [2]
  - Handle complex geometry
  - Adaptive mesh
  - High-order of accuracy and hp-adaptivity
  - Explicit semi-discrete form
- Time Integration:
  Leap-frog
  - Solving a system of equations in staggered grid points
  - Explicit 2nd order

[2] J. S. Hesthaven and T. Warburton, *Nodal Discontinuous Galerkin Methods. Algorithms, Analysis, and Applications*, Springer-Verlag, New York, 2008.

Leap-frog Discontinuous Galerkin

- Computational domain:

$$\overline{\Omega} = \cup_k T_k$$

  T_k, conforming triangular elements

- Solution on each element T_k

$$(\tilde{E}_{xk}, \tilde{E}_{yk}, \tilde{H}_{zk})$$

- Finite element space

$$V_N = \{v \in L^2(\Omega)^3 : v|_{T_k} \in P_N(T_k)\}$$

  $P_N(T_k)$: Space of polynomials of degree less than or equal to N on T_k

Leap-frog DG Full Discrete Scheme

Divide the time interval $[0, T]$ into M subintervals;

- $t^m = m\Delta t$
- Δt : Time step size
- $t^{m+1/2} = (m + \frac{1}{2})\Delta t$
- $\tilde{E}_{xk}^m = \tilde{E}_{xk}(\cdot, t^m)$, $\tilde{E}_{yk}^m = \tilde{E}_{yk}(\cdot, t^m)$ $\tilde{H}_{zk}^{m+1/2} = \tilde{H}_{zk}(\cdot, t^{m+1/2})$.

Find $(\tilde{E}_{x_k}^{m+1}, \tilde{E}_{y_k}^{m+1}, \tilde{H}_{z_k}^{m+1/2}) \in V_N$ such that, $\forall (u_k, v_k, w_k) \in V_N$,

$$\begin{aligned}
&\left(\epsilon_{xx}\frac{\tilde{E}_{x_k}^{m+1} - \tilde{E}_{x_k}^{m}}{\Delta t} + \epsilon_{xy}\frac{\tilde{E}_{y_k}^{m+1} - \tilde{E}_{y_k}^{m}}{\Delta t}, u_k\right)_{T_k} \\
&= \left(\partial_y \tilde{H}_{z_k}^{m+1/2}, u_k\right)_{T_k} + \left(\frac{-n_y}{Z^+ + Z^-}(Z^+[\tilde{H}_z^{m+1/2}]\right. \\
&\quad \left. -\alpha(n_x[\tilde{E}_y^m] - n_y[\tilde{E}_x^m])), u_k\right)_{\partial T_k}, \qquad (1)
\end{aligned}$$

Leap-frog DG Full discrete scheme

$$\left(\epsilon_{yx}\frac{\tilde{E}_{x_k}^{m+1}-\tilde{E}_{x_k}^{m}}{\Delta t}+\epsilon_{yy}\frac{\tilde{E}_{y_k}^{m+1}-\tilde{E}_{y_k}^{m}}{\Delta t},v_k\right)_{T_k}$$
$$=\left(\partial_x\tilde{H}_{z_k}^{m+1/2},v_k\right)_{T_k}+\left(\frac{n_x}{Z^+ + Z^-}(Z^+[\tilde{H}_z^{m+1/2}]\right.$$
$$\left.-\alpha(n_x[\tilde{E}_y^m]-n_y[\tilde{E}_x^m]),v_k\right)_{\partial T_k}, \quad (2)$$

$$\left(\mu\frac{\tilde{H}_{z_k}^{m+3/2}-\tilde{H}_{z_k}^{m+1/2}}{\Delta t},w_k\right)_{T_k}$$
$$=\left(\partial_y\tilde{E}_{x_k}^{m+1}-\partial_x\tilde{E}_{y_k}^{m+1},w_k\right)_{T_k}+\left(\frac{1}{Y^+ + Y^-}(Y^+\right.$$
$$\left.(n_x[\tilde{E}_y^{m+1}]-n_y[\tilde{E}_x^{m+1}])-\alpha[\tilde{H}_z^{m+1/2}]),w_k\right)_{\partial T_k}, \quad (3)$$

Numerical Flux

- Flux : [3]
  Coupling between the elements
- $\alpha \in [0, 1]$: Control dissipation
  - $\alpha = 0$; Dissipative central flux
  - $\alpha = 1$; Upwind flux
- Jump in the field values across the interfaces of the elements

$$[\tilde{E}] = \tilde{E}^{-} - \tilde{E}^{+}$$

$$[\tilde{H}] = \tilde{H}^{-} - \tilde{H}^{+}$$

  - Superscript "$+$": Neighbouring element
  - Superscript "$-$": Local cell

[3] M. Konig, K. Busch and J. Niegemann, "The Discontinuous Galerkin Time-Domain method for Maxwell's equations with anisotropic materials", Photon. Nanostruct. Fundam. Appl. 8(4), pp. 303-309, 2010.

- Speed with which the a wave travels along the direction of the unit normal, n

$$c^{\pm} = \sqrt{\frac{n^T \epsilon^{\pm} n}{\mu^{\pm} \det(\epsilon^{\pm})}}$$

- Cell-impedances

$$Z^{\pm} = \mu^{\pm} c^{\pm}$$

- Cell-conductances

$$Y^{\pm} = \left(Z^{\pm}\right)^{-1}$$

If

$$\Delta t < \frac{\min\{\bar{\epsilon}, \bar{\mu}\}}{\max\{C_E, C_H\}} \min\{h_k\}$$

where

$$C_E = \frac{1}{2} C_{inv} + C_{trace}^2 N^2 \left(1 + \frac{\alpha}{2\min\{Z_k\}} + \frac{\beta_1}{2\min\{Z_k\}} + \frac{\beta_2}{2}\right)$$

$$C_H = \frac{1}{2} C_{inv} + C_{trace}^2 N^2 \left(2 + \frac{\alpha}{2\min\{Y_k\}} + \frac{\beta_2 \beta_3}{2\min\{Y_k\}} + \frac{\beta_2}{2}\right)$$

and $\beta_1 = \alpha, \beta_2 = 0$ for PEC,
$\beta_1 = 0, \beta_2 = 1$, $\beta_3 = \alpha$ for PMC,
and $\beta_1 = \beta_2 = \frac{1}{2}$, $\beta_3 = 1$ for Silver-Müller boundary conditions.
the method is stable.

Leap-frog DG Method

Theorem

Under the CFL condition:

$$\Delta t < \frac{\min\{\bar{\epsilon}, \bar{\mu}\}}{\max\{C_E, C_H\}} \min\{h_k\}$$

and the sufficient regularity of electromagnetic fields,

$$\max_{m \geq 1}(\|E^m - \tilde{E}^m\| + \|H^{m+1/2} - \tilde{H}^{m+1/2}\|) \leq$$
$$(\Delta t^2 + h^{N+\alpha})(\|E^0 - \tilde{E}^0\| + \|H^{1/2} - \tilde{H}^{1/2}\|).$$

Numerical Results

- Computational domain :
  Unit square $\Omega = [-1, 1]^2$

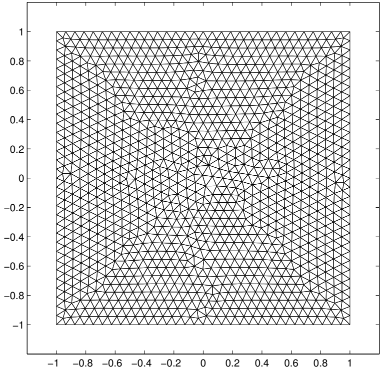

Figure: Nonuniform mesh of the unit square for K = 2310 triangles

The field distribution within the unitary cavity is given by

$$E_x(x,y,t) = \frac{-\pi}{\omega\epsilon_{xx}}.\cos(\pi x).\sin(\pi y).\sin(\omega t)$$

$$E_y(x,y,t) = \frac{\pi}{\omega\epsilon_{yy}}.\sin(\pi x).\cos(\pi y).\sin(\omega t)$$

$$H_z(x,y,t) = cos(\pi x).\cos(\pi y).\cos(\omega t),$$

where

$$\omega = \pi\sqrt{\frac{1}{\epsilon_{xx}} + \frac{1}{\epsilon_{yy}}}$$

The permittivity tensor ϵ is diagonal and characterized by

$$\epsilon' = \begin{pmatrix} \epsilon_{xx} & 0 \\ 0 & \epsilon_{yy} \end{pmatrix}$$

Numerical Results

Consider symmetric positive definite with non-vanishing off-diagonal elements

$$\epsilon = \begin{pmatrix} \epsilon_{xx} & \epsilon_{xy} \\ \epsilon_{yx} & \epsilon_{yy} \end{pmatrix}$$

Eigenvalue decomposition of ϵ

$$\epsilon = \mathcal{R}(\phi)\epsilon' \mathcal{R}(\phi)^T,$$

where $\underline{\epsilon}$ is a diagonal matrix whose diagonal entries are the eigenvalues of ϵ.

Rotation angel:

$$\phi = \arccos\left(\sqrt{\frac{\epsilon_{xx} - \lambda_2}{\lambda_1 - \lambda_2}}\right).$$

- $$\epsilon = \begin{pmatrix} 5 & 1 \\ 1 & 3 \end{pmatrix}$$
- Rotation angel: $\phi = \frac{\pi}{8}$.
- Diagonal tensor :
$$\underline{\epsilon} = \begin{pmatrix} 5.4142 & 0 \\ 0 & 2.5858 \end{pmatrix}$$
- Boundary conditions:
  - PEC: $[\tilde{E}_x] = 2\tilde{E}_x^-$, $[\tilde{E}_y] = 2\tilde{E}_y^-$, $[\tilde{H}_z] = 0$
  - PMC: $[\tilde{E}_x] = 0$, $[\tilde{E}_y] = 0$, $[\tilde{H}_z] = 2\tilde{H}_z^-$
  - Silver-Müller
$$Z^- \tilde{H}_z^+ = n_x \tilde{E}_y^+ - n_y \tilde{E}_x^+$$
$$Z^- \tilde{H}_z^+ = (n_x \tilde{E}_y^- - n_y \tilde{E}_x^-)$$

Numerical Results

K	Error E_x	Rate E_x	Error E_y	Rate E_y	Error H_z	Rate H_z
8	1.56E-01		1.07E-01		2.27E-01	
46	6.29E-03	3.67	7.50E-03	3.04	6.13E-03	4.13
146	1.09E-03	3.04	1.44E-03	2.86	6.31E-04	3.94
568	1.30E-04	3.12	1.68E-04	3.16	4.06E-05	4.04
2310	1.62E-05	2.97	2.06E-05	2.99	2.57E-06	3.94

K	Error E_x	Rate E_x	Error E_y	Rate E_y	Error H_z	Rate H_z
8	5.33E-02		5.55E-02		1.78E-01	
46	2.46E-03	3.52	3.34E-03	3.21	3.81E-03	4.39
146	3.48E-04	3.38	4.35E-04	3.53	3.78E-04	4.00
568	2.41E-05	3.93	2.93E-05	3.97	2.48E-05	4.01
2310	1.49E-06	3.96	1.85E-06	3.94	1.50E-06	4.00

Numerical Results

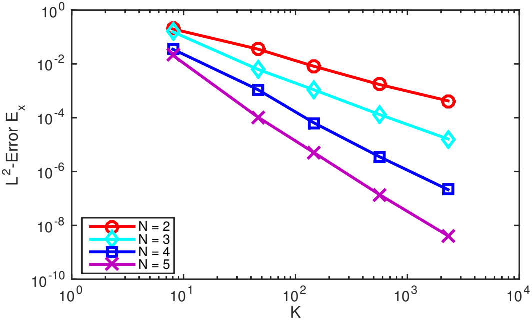

Figure: Convergence in space: N order of convergency of E_x in the case of central flux ($\alpha = 0$), for different polynomial orders.

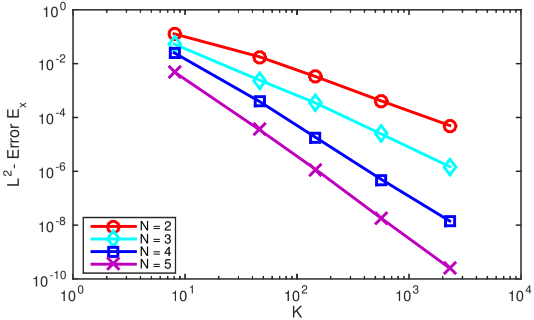

Figure: Convergence in space: N order of convergency of E_x in the case of upwind flux ($\alpha = 1$), for different polynomial orders.

Numerical Results

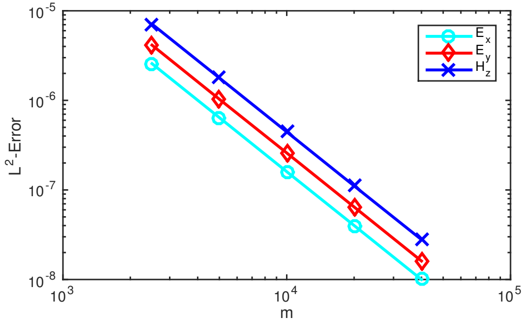

Figure: Convergence in time: 2nd order convergence of E_x, E_y and H_z when $\alpha = 1$ (upwind flux) and PEC boundary conditions.

Numerical Results

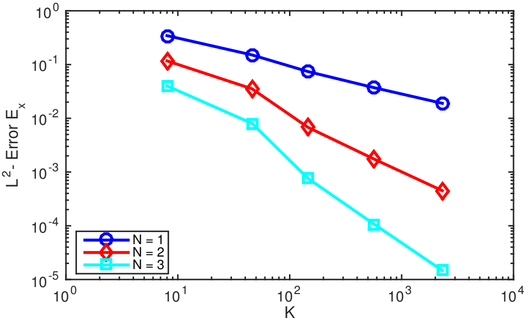

Figure: Convergence in space: N order of convergency of E_x in the case of central flux ($\alpha = 0$), for different polynomial orders.

Numerical Results

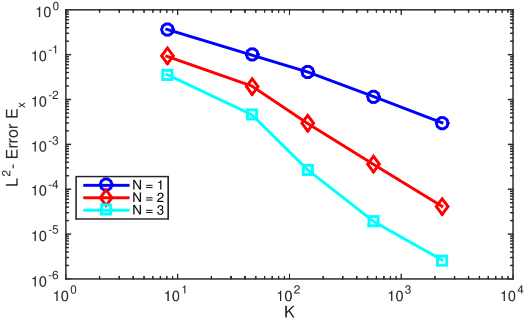

Figure: Convergence in space: N order of convergency of E_x in the case of upwind flux ($\alpha = 1$), for different polynomial orders.

Conclusion

- Fully explicit leap-frog DG scheme for solving time dependent Maxwell's equations in anisotropic media which is in our application of interest.
- Conditionally stable
- Convergent:
- Optimal order of convergence $\mathcal{O}(h^{N+1}, \Delta t^2)$ for upwind flux

Acknowledgments

This work was supported by the Centro de Matemática da Universidade de Coimbra (CMUC), funded by the European Regional Development Fund through the program COMPETE, and by the Portuguese Government through the FCT - Fundação para a Ciência e a Tecnologia under the projects PEst-C/MAT/UI0324/2013 and PTDC/SAU-ENB/119132/2010 and under the BD grant SFRH/BD/51860/2012.